ELSEVIER

J. Non-Newtonian Fluid Mech. 112 (2003) 1–26

Journal of Non-Newtonian Fluid Mechanics

www.elsevier.com/locate/jnnfm

Turbulent flow of a viscoelastic shear-thinning liquid through a plane sudden expansion of modest aspect ratio

R.J. Poole, M.P. Escudier*

Department of Engineering, Mechanical Engineering, University of Liverpool, Brownlow Hill, Liverpool L69 3GH, UK

Received 20 December 2002; received in revised form 3 February 2003

Abstract

An experimental investigation is reported of turbulent flow of a 0.125% polyacrylamide (PAA) solution, a shear-thinning and viscoelastic liquid, through a plane sudden expansion of expansion ratio $R = D/d = 4$ and aspect ratio $A = w/h = 5.33$. A Newtonian fluid flow through the same geometry has been reported previously [Phys. Fluids 14 (2002) 3641] and limited results from that study are included here for comparative purposes. It is well known, for Newtonian fluids at least, that plane sudden expansions with R greater than 1.5 produce asymmetric flows. For the viscoelastic fluid flow, this asymmetry was initially ($x/d < 6$) reduced but not eliminated and the flow found to be highly three dimensional and complex. Results are reported at three spanwise locations to highlight this three dimensionality.

Keywords: Viscoelastic; Shear thinning; Turbulent; Plane sudden expansion

1. Introduction

The turbulent flow of fluids through sudden expansions has both fundamental scientific interest and numerous practical applications: such flows occur, for example, in pipe-flow systems in the chemical, pharmaceutical and petroleum industries, in air-conditioning ducts, around buildings, in dump combusters and in fluidic devices. As far as Newtonian fluids are concerned, much of the fundamental understanding of turbulent free shear layers and separated internal flows has resulted from investigations of the flow through a sudden expansion or over a backward-facing step. Indeed, the developers of turbulence codes have relied heavily on these flows, and in particular the backward-facing step geometry, to validate and improve their simulations.

Although many naturally occurring fluids, and the majority of synthetic fluids such as those encountered in the food, processing and chemical industries, are non-Newtonian in character, the existing literature

* Corresponding author. Tel.: +44-151-794-4804; fax: +44-151-794-4848.
E-mail address: escudier@liv.ac.uk (M.P. Escudier).

0377-0257/03/$ – see front matter
doi:10.1016/S0377-0257(03)00058-2

Nomenclature

a	constant in Carreau–Yasuda model
A	aspect ratio (w/h)
b	constant in power-law variation for normal-stress variation
c	polymer concentration (g/m^3)
d	duct height at inlet (m)
D	downstream duct height (m)
De	Deborah number ($\equiv \lambda/T_{CH}$)
h	step height (m)
m	power-law index in power-law variation for normal-stress variation
M	molecular weight (g/mol)
n	power-law index
N_1	first normal-stress difference (Pa)
$\dot{Q}_A$	apparent flowrate determined by numerical integration (m^3/s)
$\dot{Q}_F$	flowrate from flowmeter (m^3/s)
R	expansion ratio (D/d)
R_G	gas constant (J/mol K)
Re	Reynolds number ($\equiv \rho h U_B/\mu_{SEP}$)
T	temperature (K)
T_{CH}	characteristic time of deformation process (s)
U	mean streamwise velocity (m/s)
u'	streamwise turbulence intensity (m/s)
U_B	bulk mean velocity ($\dot{Q}_F/wd$) (m/s)
U_{RMAX}	maximum recirculating streamwise velocity (m/s)
$\overline{uv}$	Reynolds shear stress (m^2/s^2)
V	mean transverse velocity (m/s)
v'	transverse turbulence intensity (m/s)
w	channel width (also duct height upstream of smooth contraction) (m)
x	streamwise distance from expansion (m)
x_R	reattachment length (m)
X_R	non-dimensional reattachment length (x_R/h)
y	transverse distance from downstream duct floor (m)
z	spanwise distance from side wall (m)

Greek letters

λ	relaxation time of fluid (s)
λ_{CY}	time constant in Carreau–Yasuda model (s)
μ_0	zero-shear-rate viscosity (Pa s)
μ_{CY}	Carreau–Yasuda viscosity (Pa s)
μ_M	measured viscosity (Pa s)
μ_{SEP}	Carreau–Yasuda viscosity corresponding to shear-rate at inlet (Pa s)

μ_∞	infinite-shear-rate viscosity (Pa s)
τ	shear stress (Pa)

Subscripts

L	lower recirculation region
max	maximum
U	upper recirculation region
0	freestream

is almost devoid of both experimental and computational studies of the turbulent flow of non-Newtonian fluids in any other situation other than fully-developed pipe or duct flow. Hitherto research into the turbulent flow of non-Newtonian liquids has been concerned to a large extent with the important, but still not completely understood, phenomenon of drag reduction in pipe or duct flow. In a recent experimental study, the present authors [1,2] investigated the turbulent flow of a range of non-Newtonian liquids through a plane sudden expansion of expansion ratio 1.43, which acts essentially as a double backward-facing step. The study reported here extends this work by examining the turbulent flow of a strongly viscoelastic liquid through a plane sudden expansion with an expansion ratio of 4.

For Newtonian fluid flows through plane sudden expansions a key geometric parameter is the expansion ratio R ($=D/d$), where D is the downstream channel height and d the inlet height. In the first systematic study of the influence of R, Abbott and Kline [3] used a modified hot-film anemometer and a dye-injection technique to observe flow patterns for different expansions covering the range $1.125 < R < 5$. They found that for $R > 1.5$ the flow became asymmetric with two recirculation zones of unequal length on opposite sides of the duct, while below this value the flow approached that for a double backward-facing step configuration with symmetrical regions of recirculation. This asymmetry appears to be independent of the aspect ratio $A = w/h =$ channel width/step height. Abbott and Kline's findings have been confirmed by other investigators and it is now generally accepted that flow through a plane sudden expansion must be divided into two regimes depending on the expansion ratio. In most previous work, the aspect ratio ($A = w/h$, w being the duct width and h the step height) has been either less than 1 or greater than 10. In practical applications, the aspect ratio is more likely to fall in the range 1–10 and in the present work the value chosen was 5.33. Since the time of Abbott and Kline's [3] work, a considerable literature has developed devoted to the subject of turbulent flow of a Newtonian fluid over a backward-facing step (see the review of Eaton and Johnson [4] or the recent paper of Poole and Escudier [1]) whereas investigations for the asymmetric ($R > 1.5$) configuration are much more limited [5]. For comparative purposes, limited results are included from Escudier et al. [5] for turbulent flow of water through the same geometry as for the viscoelastic liquid. They found that for water not only was the mean flow strongly asymmetric, but integration of the mean streamwise velocity profiles revealed departures from two dimensionality of up to 20% (based upon apparent flowrate) along the centreplane of expansion duct.

In viscoelastic fluid flows, at least two non-dimensional groups must be defined to characterise the flow. As in classical Newtonian fluid mechanics, a Reynolds number ($Re \equiv \rho h U_B/\mu_{SEP}$) provides a measure of the inertial to viscous forces in the flow and its precise definition is only complicated for viscoelastic fluid flows if the viscosity, as in the current study, is not constant. In addition, a Deborah number defines the degree of viscoelasticity of the flow. This is defined as $De \equiv \lambda/T_{CH}$, where T_{CH} is a characteristic

time of the deformation process being observed (i.e. the flow) and λ is a characteristic time of the fluid. For a Newtonian fluid flow, the Deborah number is equal to zero.

We could find no published papers dealing with turbulent non-Newtonian liquid flows through plane sudden expansions. There are, however, a handful of papers which investigate laminar flows of these liquids, primarily at very low Reynolds numbers (estimated as $0.1 < Re < 10$ based on a constant viscosity). Townsend and Walters [6] used flow visualisation to observe the flowfield downstream of both a two- and three-dimensional sudden expansion for the flow of a 0.15% aqueous solution of polyacrylamide (PAA) at low *Re* (estimated as 10) and Deborah number (estimated as 1). They concluded that the viscoelasticity of the polymer solution prevented vortex activity and resulted in any recirculating fluid being pushed into the corners of the expansion. The results of a theoretical model developed to simulate the flowfield numerically were in good physical agreement with the observed flow visualisation but only qualitative in nature due to the lack of quantitative rheological and velocity data. The experiments of Townsend and Walters were also used as the basis for comparison in the numerical simulation work of Baloch et al. [9] for $Re = 1$, 2 and 4 at Deborah numbers of 1 and 2. Expansion flows were modelled in two and three dimensions using a class of constitutive models due to Phan-Thien and Tanner [10]. Once again, good qualitative agreement was seen with the experimental visualisations and the conclusion again drawn was that viscoelasticity suppresses vortex activity and that this suppression is linked to the phenomenon of die swell.

The numerical works of Darwish et al. [7] ($Re = 0.1$, $De = 0$, 0.8 and 2.4) and later Missirlis et al. [8] ($Re = 0.1$, $De = 0$, 1.2 and 3) are very similar. Both use a finite-volume technique to simulate the flow of a viscoelastic liquid through a two-dimensional 4:1 plane sudden expansion. Neither validate their work by comparison with experimental data but infer verification using grid refinement to obtain grid-independent results. Missirlis et al. show that the suppression of vortex activity is related to the Deborah number. They show that if *De* is increased beyond a critical value of 3.0, the recirculation zone is completely eliminated.

The objective of the present study is to examine the combined influence of shear thinning and viscoelasticity on the turbulent reattachment process downstream of a plane sudden expansion. A 0.125% concentration of polyacrylamide in water was chosen as this results in a liquid which is both highly shear thinning and highly viscoelastic.

2. Experimental rig and instrumentation

The flow loop used for the present experiments was a modified version of that used by Poole and Escudier [5] for their backward-facing step investigation. The backward-facing step arrangement [5] was replaced by a plane sudden expansion installed 9.6 m from the inlet connection. The key dimensions are given in Fig. 1. The duct width w remained 80 mm throughout, the inlet height d was 10 mm, the step height h was 15 mm and the downstream duct height D was 40 mm. These dimensions produce an expansion ratio $R = D/d = 4$ and an aspect ratio $A = w/h = 5.33$. By choosing $R > 1.5$ it was anticipated that the flow would be asymmetrical if the Abbott and Kline [3] criterion also applies to non-Newtonian fluid flow.

The expansion was preceded by a short (53.5 mm in length), smooth contraction (40 mm concave radius followed by 20 mm convex radius) which for the higher Reynolds number flows led to a distribution of velocity at the plane of the sudden expansion which was practically uniform and of low turbulence

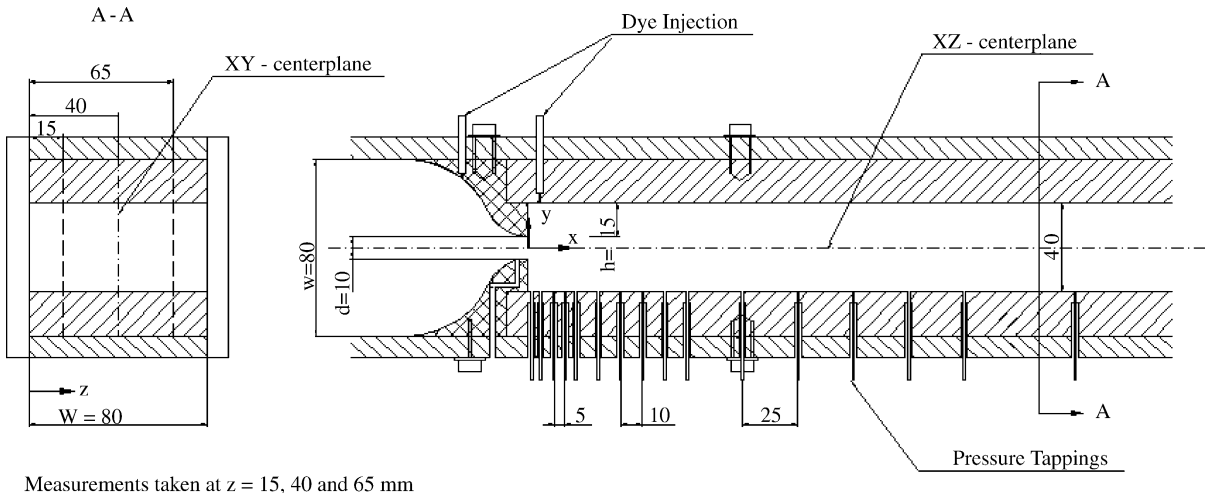

Fig. 1. Plane sudden expansion geometry, dimensions in mm.

intensity. The side walls of the expansion were made of borosilicate glass to permit velocity measurements using a laser Doppler anemometer (LDA). Distributions of mean velocity and turbulence structure were obtained from traverses at 12 streamwise locations (corresponding to x/d values of 0, 1, 2, 3, 4, 5, 6, 7, 10, 12, 15 and 18) at three spanwise locations, $z/d = 4$, 1.5 and 6.5, which correspond to the *XY*-centreplane of the duct and two parallel planes one step height from each of the side walls (Fig. 1). The region below $y/h = 0.33$ was inaccessible to the LDA beams in the *YZ*-plane and so no transverse turbulence intensities or Reynolds shear stresses could be reported below this height.

A Dantec Fibreflow laser Doppler anemometer system was used for the velocity and turbulence measurements and comprised a Dantec 60X10 probe and a Dantec 55X12 beam expander in conjunction with two Dantec Burst Spectrum Analyzer signal processors (one model 57N10, the other model 57N20). The beam separation at the front lens was 51.5 mm and the lens focal length 160 mm (corresponding to an included half angle of 9.14°) which produces a measurement volume with principal axis of length 0.21 mm and diameter 20 μm. In view of the small diameter of the measuring volume, no correction was applied for the effect of velocity-gradient broadening. The streamwise and transverse velocity values were collected in coincidence to enable the Reynolds shear stress values to be estimated. As recommended by Tropea [12], transit-time weighting was used to correct the velocity measurements for the effects of velocity bias. Nominally, 10,000 velocity samples were collected which resulted in a maximum relative statistical error, for a 95% confidence interval, of approximately 0.5% in the mean velocity and 1.4% in the turbulence intensity [13]. The total uncertainty in the mean velocity is estimated to be in the range 3–4% and in the range 6–7% for the turbulence intensities.

As shown in Fig. 1, 19 pressure tappings of 1 mm diameter were provided along the *XY*-centerplane of the expansion to allow the wall-pressure variation to be measured. The tappings were connected to 2 mm i.d. clear vinyl tubing, filled with deionised water, linking each in turn via a series of valves to a Validyne differential pressure transducer (model DP15-26). Flow rates were measured using a Fischer and Porter electromagnetic flowmeter (model 10D1) incorporated in the flow loop upstream of the sudden expansion with the flowmeter output signal recorded via an Amplicon PS 30AT A/D converter.

All rheological measurements were carried out using a TA Instruments Rheolyst AR 1000N controlled-stress rheometer. A temperature of 20 °C was maintained for the rheological measurements, which was also the average temperature of the fluid for the duration of the experimental runs. Control of the temperature of the sample to within ±0.1 °C is achieved in the rheometer via a plate using the Peltier effect.

3. Rheology of working fluid

The working fluid used in this investigation was a 0.125% concentration of polyacrylamide, Separan AP273 E supplied by SNF, UK Limited. The solvent used was filtered tap water with 100 ppm of 40% formaldehyde solution (i.e. 4×10^{-3}% concentration) added to retard bacterial degradation. Approximately, 0.25 gm of Timiron seeding particles (average size 5 μm) were added to the fluid (total volume of fluid 575 l) to improve the LDA signal quality.

PAA was chosen as the working fluid as it is highly viscoelastic, is optically transparent (thereby permitting LDA measurements) and has been used extensively in previous investigations in the same laboratory [2,11,14] and elsewhere [15,16]. According to Walters et al. [17] PAA is 'very flexible' in its molecular structure and this gives rise to its increased elastic properties compared to other water-soluble polymers such as xanthan gum and carboxymethylcellulose. The average molecular weight for the PAA used in this study, ascertained using gel-phase chromatography, was determined to be 1.94×10^6 kg/kmol with a polydispersity of 1.05. The flow curve (i.e. viscosity versus shear rate) for PAA is shown in Fig. 2

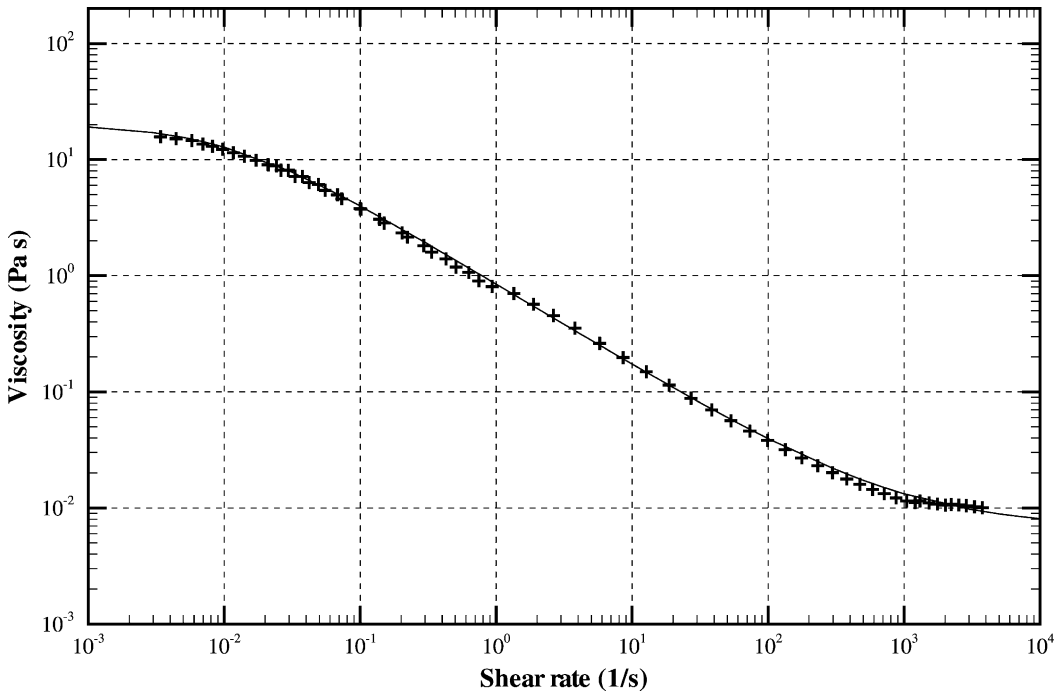

Fig. 2. Viscosity vs. shear rate for 0.125% polyacrylamide (including Carreau–Yasuda fit).

Table 1
Carreau–Yasuda model parameters

μ_0 (Pa s)	μ_∞ ($\times 10^3$ Pa s)	λ_{CY} (s)	n	a
20.4	6.82	90.3	0.707	0.978

together with the corresponding Carreau–Yasuda model fit:

$$\mu_{CY} = \mu_\infty + \frac{\mu_0 - \mu_\infty}{(1 + (\lambda_{CY}\dot{\gamma})^a)^{n/a}},$$

where μ_0 is the zero-shear-rate viscosity, μ_∞ the infinite-shear-rate viscosity, λ_{CY} is a time constant, n is the power-law index and a is a parameter introduced by Yasuda et al. [18]. The model parameters, which are listed in Table 1, were determined using the fitting procedure (in essence minimisation of the standard deviation, $(1 - \mu_M/\mu_{CY})^2$) outlined in Escudier et al. [19]. The measured variation of the first normal-stress difference N_1, which is a good indicator of the level of elasticity of a fluid, versus shear stress, τ, is shown in Fig. 3. A power-law fit to the N_1/τ data has been included in Fig. 3 and the parameters are listed in Table 2. In the measured range, the recoverable shear $N_1/2\tau$ is much greater than 0.5 indicating a highly elastic liquid [20].

To estimate a Deborah number ($De \equiv \lambda/T_{CH}$) for the flow it is necessary to estimate both a characteristic relaxation time for the fluid (λ) and for the deformation process (T_{CH}). To estimate a *relevant* relaxation time for the fluid is non-trivial but it is apparent that regardless of λ, *De* is likely to be very large. A characteristic time for the flow can be taken as the step height divided by the bulk velocity, i.e.

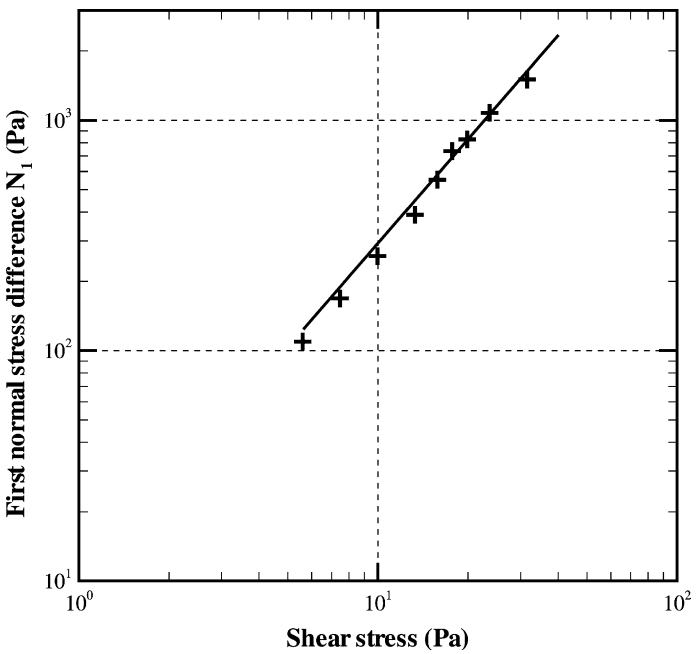

Fig. 3. First normal-stress difference vs. shear stress for 0.125% polyacrylamide.

Table 2
Power-law parameters for normal-stress variation

Fluid	Range of τ (Pa)	Power-law parameters ($N_1 = b\tau^m$)	
		b	m
0.125%	5.5–40	11.2	1.43

$T_{CH} = h/U_B = 2.1$ ms. As the PAA used in this study is highly viscoelastic (based on recoverable shear) it is likely that a characteristic relaxation time would be at least of the order of 0.1 s [21] (the numerical works of [7–9] use relaxation times of the order of 1 s) and this gives a Deborah number of about 50. If the longest possible relaxation time of the fluid were used (using the method of Tam and Tui [22], $\lambda = (\mu_0 - \mu_\infty)M/cR_GT \approx 10$ s), then the Deborah number would be about 5000. A Deborah number of this order means that the flow will exhibit significant elastic effects.

4. Results and discussion

All data presented here refer to a Reynolds number of 13,700 based on the mean bulk velocity at the expansion, $U_B = 7.16$ m/s, the step height, $h = 15$ mm, and a viscosity estimated from the Carreau–Yasuda model using the shear rate at inlet. This shear rate was estimated assuming a linear variation between the mean velocity at the first measuring point (0.5 mm from wall) and the no-slip condition at the wall.

4.1. Wall-pressure variation

For water flow it was found [5] that the shorter region of recirculation was equally likely to occur on the top and bottom walls on start-up, i.e. there was no preferred physical side for the shorter reattachment length. Also because the flow 'switched', although the pressure tappings were physically on the lower wall, both lower and 'upper' wall pressures could be measured. In contrast, the PAA flow did not 'switch' on start-up (i.e. the shorter recirculation region always occurred on the same physical wall) and, because pressure tappings were only located on the lower-wall, only the lower-wall-pressure values could be measured. This preferred structure of the PAA flow might suggest that, along the *XY*-centreplane at least, the top-to-bottom asymmetry seen in Newtonian flows is absent. As will be seen in what follows, the flow is in fact asymmetric, although the asymmetry is reduced in the near vicinity of the expansion. This preference or 'stability' of the flow could be related in some way to the long-range 'memory' effects that we have observed previously in our laboratory for viscoelastic liquids: these include pipe-flow velocity profiles that became asymmetric during transition [23] and in fully-developed square duct flow (in the absence of a flow straightner) where a large component of swirl was observed 13 m from the inlet bend [24]. Another possibility is that this behaviour is caused by a slight geometric imperfection the effects of which are accentuated by high levels of viscoelasticity but attenuated for viscous flows.

The wall-pressure variation for PAA on the lower wall is shown in Fig. 4 together with the lower and upper-wall-pressure variation for water. The variation for PAA is similar to the upper-wall variation for the Newtonian fluid except that immediately after the step, the pressure coefficient is positive in the viscoelastic case, perhaps an indication that the measurement represents a combination of the static pressure and the first normal-stress difference N_1 [25].

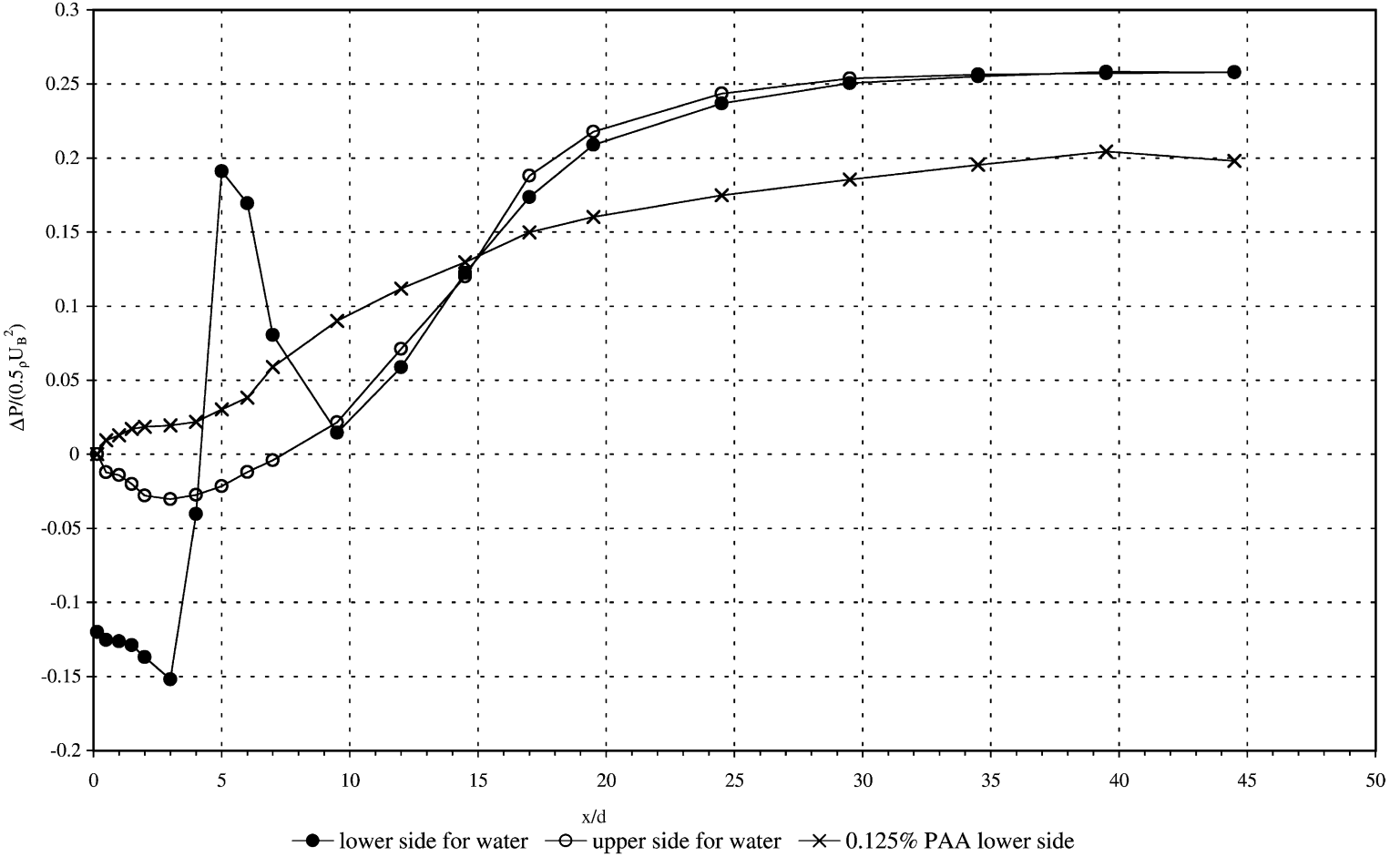

Fig. 4. Wall-pressure variation.

4.2. Mean streamwise velocity profiles, U/U_B

The 'stability' of the flow seen in terms of wall-pressure variation is partly confirmed by the mean streamwise velocity profiles of Fig. 5a and b. The differences to the water flow (Fig. 6) are extreme and it is clear that the flowfield is fundamentally different. Along the *XY*-centreplane, the top-to-bottom asymmetry seen for the Newtonian fluid flows is diminished but not eliminated as is evident from the absence of recirculating fluid above the high-velocity core (i.e. $y/D > 0.5$) whereas recirculation is evident below the core. As the flow along the *XY*-centreplane progresses, the high-velocity core spreads out, almost symmetrically, until, by $x/d = 6$, the flow is uniform over nearly 50% of the duct between $y/D = 0.2$ and 0.65. Downstream of $x/d = 6$ a small recirculation region is formed (inferred from negative mean velocities near the wall) above the high-velocity core and, as a consequence, the top-to-bottom asymmetry is accentuated rather than diminished with downstream distance until by $x/d = 18$ the profiles are highly asymmetric.

The off-centreplane data, at $z = 15$ and 65 mm, are also in marked contrast to the water flow. The side-to-side asymmetry seen in the Newtonian case, at least upstream of $x/d = 12$, is largely absent and the flow is practically symmetrical about the *XY*-centreplane. Although the flow is symmetrical, it is far from two dimensional and the profiles in these two planes are more akin to the water profiles (Fig. 6) than the *XY*-centreplane data for PAA. The $z = 15$ and 65 mm profiles are both asymmetric from top-to-bottom with recirculating fluid seen in both regions. The reattachment length on the lower wall is about 5 step heights, an increase of about 60% compared to the average value for the water flow, i.e. 3.1 step heights. The flow along the *XY*-centreplane reattaches on the lower wall at about four step heights, an increase compared to the Newtonian fluid flow of about 30%. In the upper region, the flow in the *XY*-centreplane is always in the positive streamwise direction until approximately $x/d = 6$, where near the wall, negative velocities occur and a recirculation region forms. The $z = 15$ and 65 mm profiles reattach at about 11 step heights, comparable to the average value for the water flow.

To further investigate flow two dimensionality, each of the mean streamwise velocity profiles was integrated numerically to produce values for the apparent flowrate $\dot{Q}_A$. These values, normalised by the true flowrate measured using the flowmeter, $\dot{Q}_F$, are plotted in Fig. 7. Also plotted is the normalised average of the three apparent flowrates as a means of gross comparison. As might be expected from visual inspection of the velocity profiles, the flowrate inferred from the data along the *XY*-centreplane is much greater than that corresponding to the $z = 15$ and 65 mm profiles. The apparent flowrate for the centreplane increases with downstream distance reaching a value almost three times greater than the true flowrate at $x/d = 7$. Similar effects have been observed previously for flow over a backward-facing step: for the laminar flow of 0.4% PAA [26] and turbulent flow of 0.125 and 0.175% PAA [2]. It seems likely that the increase in apparent flowrate with downstream distance from the expansion is again a normal-stress effect [2]; in this instance, a consequence of the elastic stresses in the viscoelastic liquid being free to relax after the expansion. Although the mean velocity profiles at $z = 15$ and 65 mm appear almost symmetrical about the *XY*-centreplane until $x/d = 12$, the values of $\dot{Q}_A/\dot{Q}_F$ show that symmetry is only maintained in the near vicinity of the expansion ($x/d < 5$). In the lower recirculation region, the flow is almost two dimensional (see Fig. 5a) whereas elsewhere it is strongly three dimensional.

There are a number of competing influences that make interpretation of the data difficult. The fluid is highly shear thinning which, in pipe flow, tends to flatten the velocity profile. The fluid is also highly viscoelastic: the high level of N_1 not only causes the flow to expand after the expansion (as in die-swell)

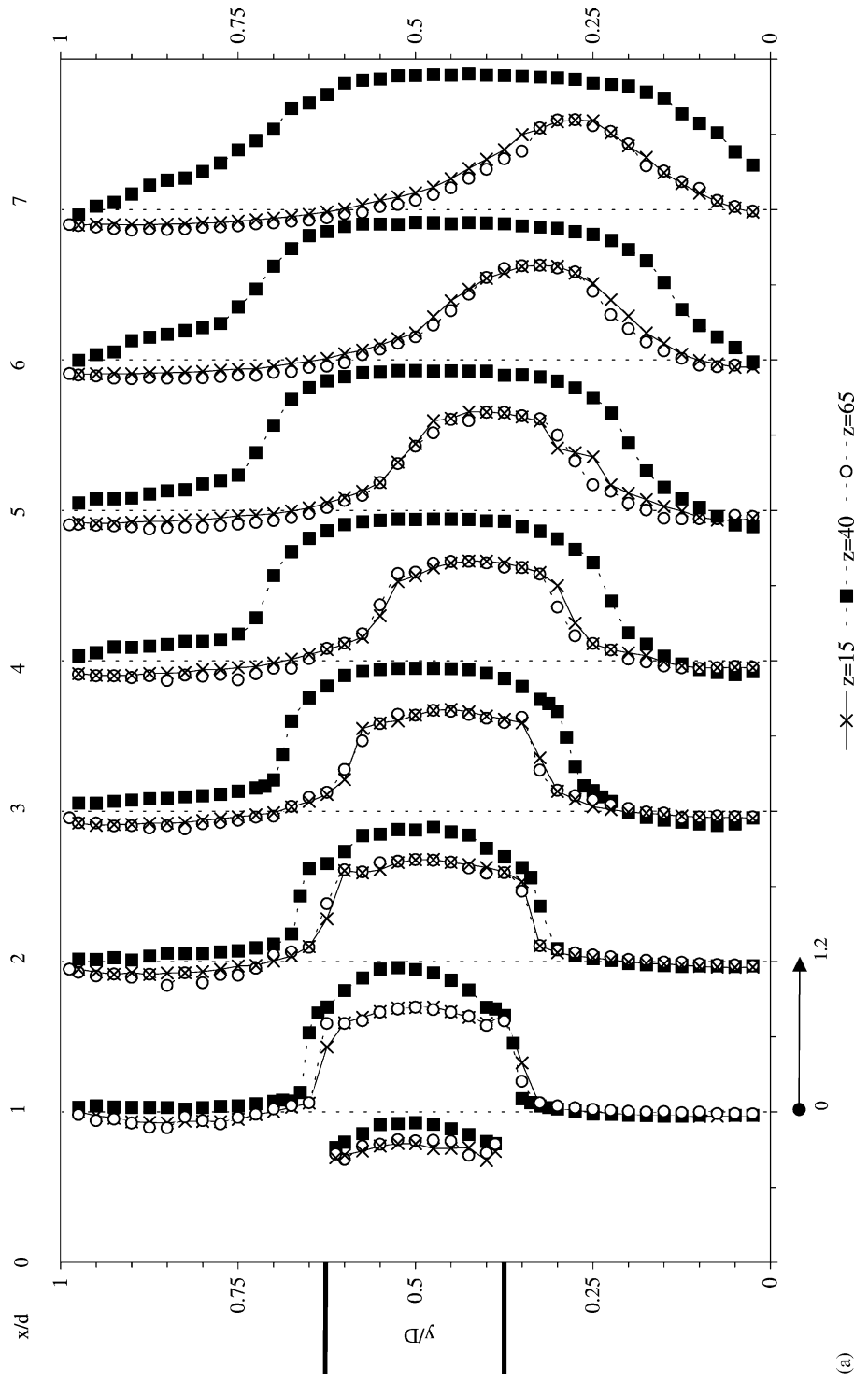

Fig. 5. (a and b) Mean streamwise velocity (U/U_B) profiles.

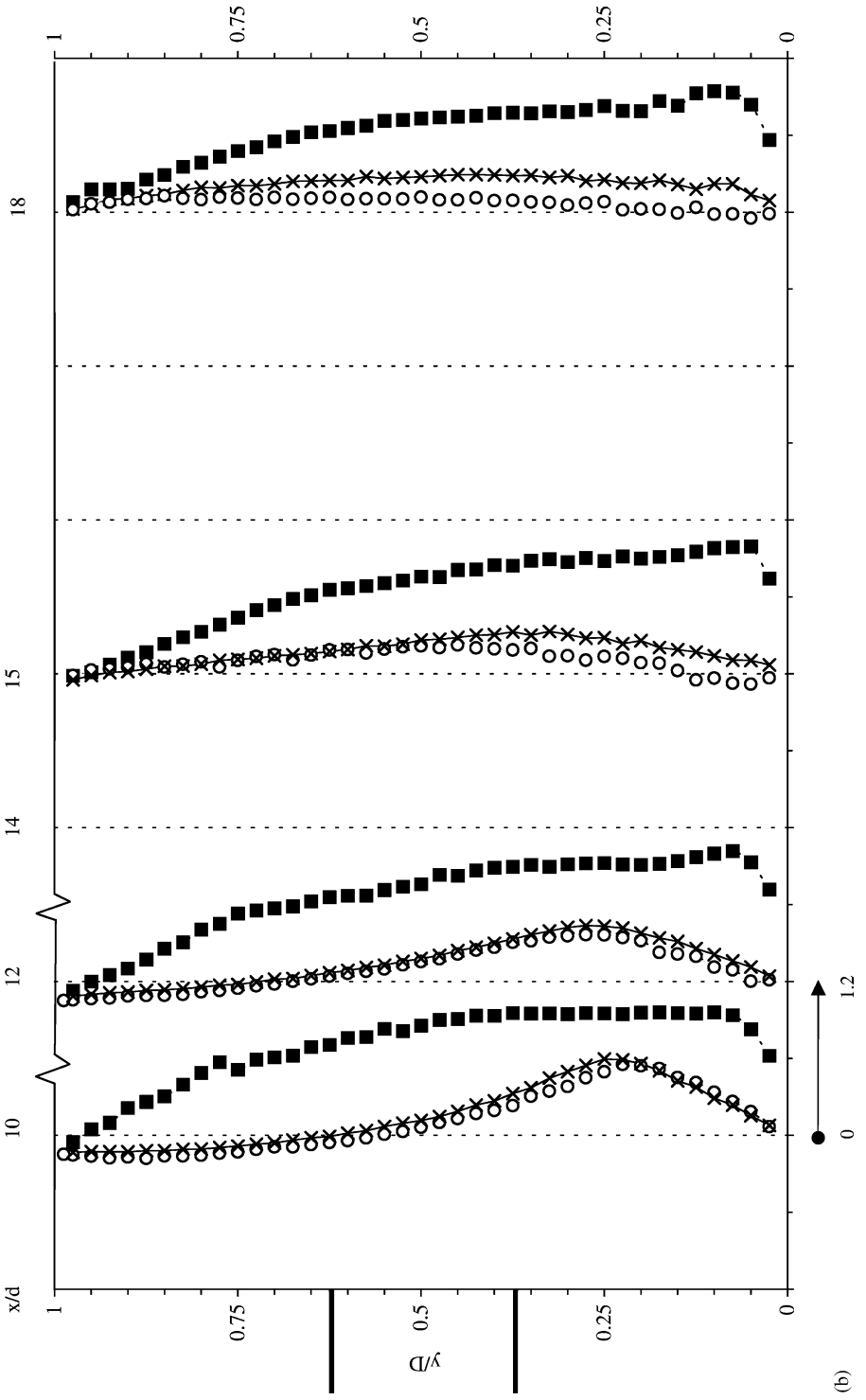

Fig. 5. (*Continued*).

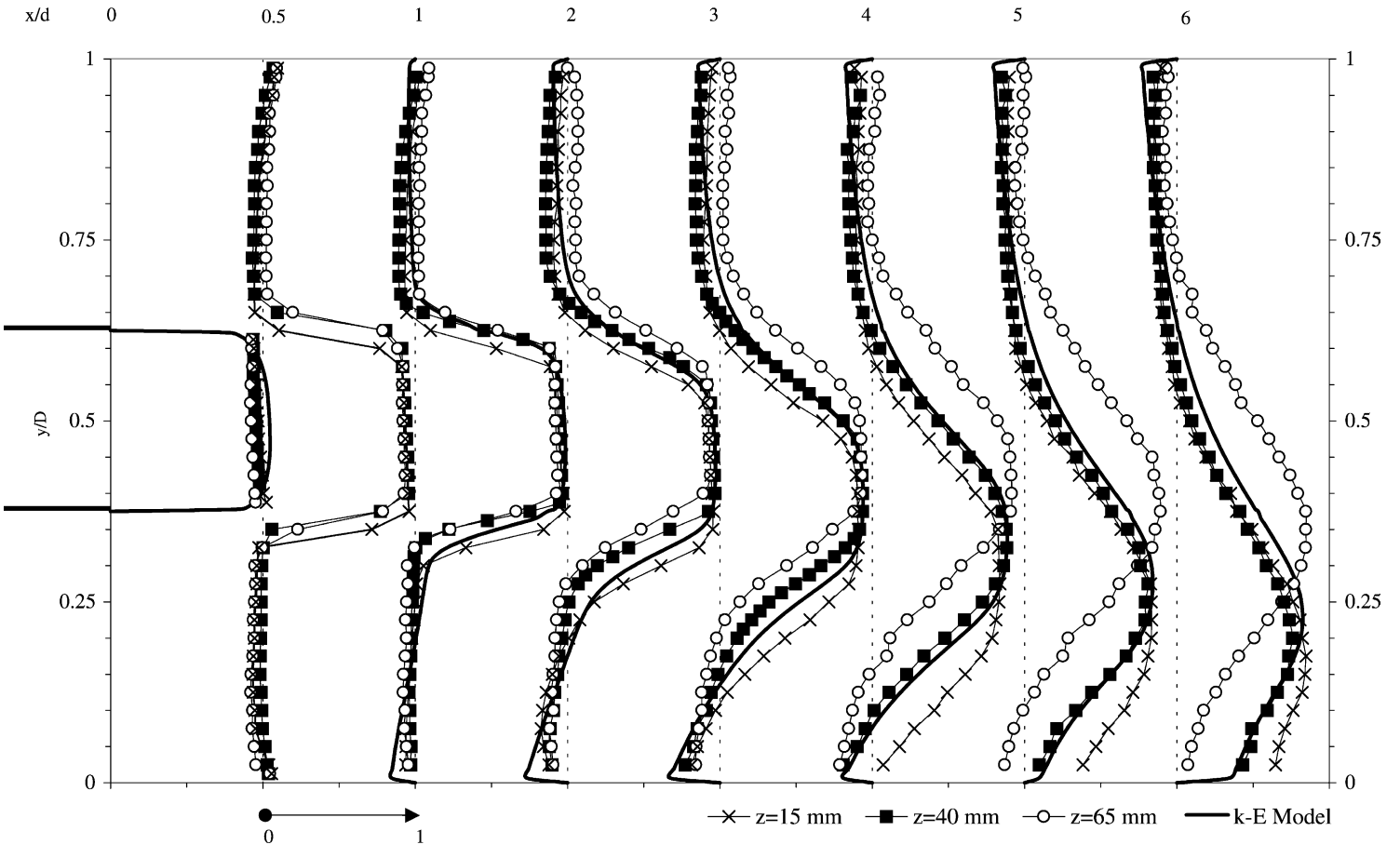

Fig. 6. Mean streamwise velocity profiles for water $Re = 87{,}250$ from [5].

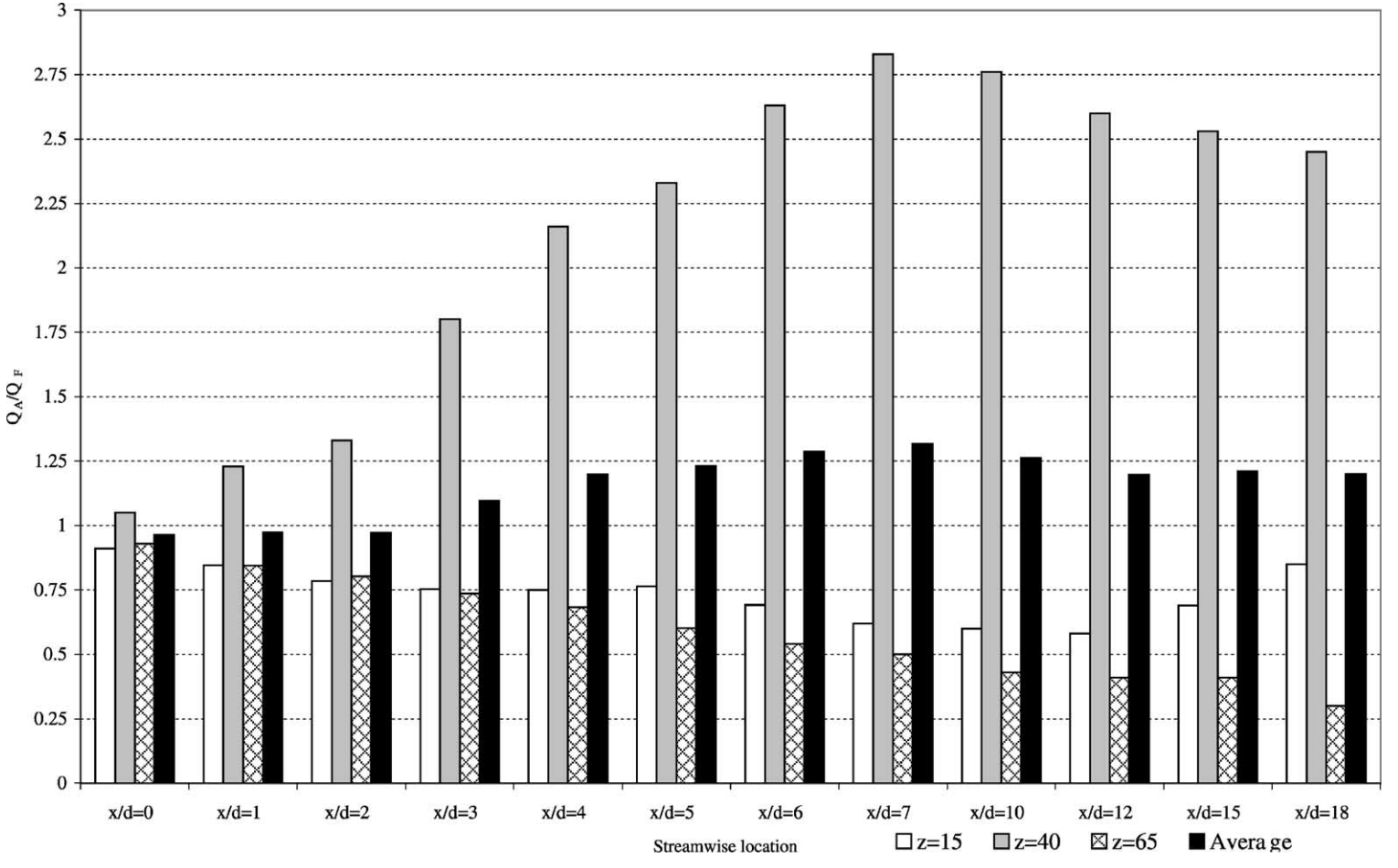

Fig. 7. Comparison between apparent flowrate from integration ($\dot{Q}_A$) and from flowmeter ($\dot{Q}_F$).

Table 3
Representative mean flow and turbulence characteristics for a plane sudden expansion, $d = 10$ mm, $D = 40$ mm

Fluid	z (mm)	$\frac{U_{\mathrm{RMAXL}}}{U_{\mathrm{B}}}$ [a]	$\frac{U_{\mathrm{RMAXU}}}{U_{\mathrm{B}}}$	$\frac{u'_{\mathrm{MAXL}}}{U_{\mathrm{B}}}$	$\frac{u'_{\mathrm{MAXU}}}{U_{\mathrm{B}}}$	$\frac{v'_{\mathrm{MAXL}}}{U_{\mathrm{B}}}$	$\frac{v'_{\mathrm{MAXU}}}{U_{\mathrm{B}}}$	$\frac{\overline{uv}_{\mathrm{MAXL}}}{U_{\mathrm{B}}^2}$	$\frac{\overline{uv}_{\mathrm{MAXU}}}{U_{\mathrm{B}}^2}$	X_{RL} (x_{RL}/h)	X_{RU} (x_{RU}/h)
Water	15	0.244	0.185	0.219	0.245	0.183	0.136	0.0235	0.0109	2.5	13.3
Water	40	0.231	0.230	0.216	0.261	0.191	0.143	0.0227	0.0119	3.1	11.5
Water	65	0.217	0.214	0.229	0.218	0.161	0.131	0.0219	0.0106	3.7	11.7
PAA	15	0.136	0.086	0.204	0.215	0.080	0.106	0.0056	0.0040	5.1	11.3
PAA	40	–	0.159	0.203	0.245	0.096	0.102	0.0104	0.0045	4.0	–
PAA	65	0.155	0.066	0.203	0.212	0.088	0.101	0.0097	0.0053	5.0	10.7

[a] Subscript MAXL indicates the maximum value in the lower recirculation region and MAXU indicates the maximum in the upper recirculation region.

but also to push fluid towards the centreplane [2]. There is a strong adverse pressure gradient causing the flow to separate from the wall and the large expansion ratio, for Newtonian fluids at least, as has been seen in previous studies [5], causes the flow to be asymmetric. Escudier et al. [5] also observed that a modest aspect ratio of 5.33 (i.e. the same as in the current study) produces a further side-to-side asymmetry for the Newtonian fluid flow. Although the high degree of three dimensionality of the flowfield is undoubtedly related to the modest aspect ratio, it is suggested that given the anisotropic nature of N_1, a much larger aspect ratio than the recommended value of 10 for a Newtonian fluid flow [27] would be needed for near two dimensionality to be approached along the *XY*-centreplane. This statement can be supported in two ways. Although characteristics of the water flow had a definite three-dimensional element (Fig. 6 and the resulting discussion in [5]), the departure from two dimensionality is mild compared to the large variations along different z profiles in the viscoelastic case. Secondly, the backward-facing step results of Poole and Escudier [2] showed that after reattachment the apparent flowrate for the viscoelastic flows along the *XY*-centreplane increased significantly despite an aspect ratio of 13.3.

The maximum recirculating velocities (documented in Table 3) show that the values for PAA are greatly reduced (>50%) compared to the water flow, much as was the case for the high (>0.125%) concentrations of PAA over a backward-facing step [2].

Downstream of $x/d = 5$ the flow situation becomes even more complex: the flow is not only asymmetric top-to-bottom but also side-to-side. Downstream of $x/d = 10$ the $z = 65$ mm profile indicates separation from the lower wall and the formation of another recirculation zone resulting in the apparent flowrate for this profile to decrease still further from an already low value until by $x/d = 18$ it is just 40% of that expected from the flowmeter.

4.3. Mean transverse velocity profiles, V/U_B

The mean transverse velocity profiles $V(y)$ (i.e. velocities in the y-direction shown in Fig. 1) of Fig. 8a and b confirm a complex three-dimensional structure. At the furthest downstream measuring location, $x/d = 18$, the maximum transverse velocity is small ($<0.05\,U_{\mathrm{B}}$) and the differences in V are slight. Upstream of $x/d = 10$ the $z = 15$ and 65 mm profiles are in close agreement with maximum negative transverse velocities of $0.13\,U_{\mathrm{B}}$ and $0.17\,U_{\mathrm{B}}$, respectively.

Along the *XY*-centreplane, the reduced asymmetry compared to the water flow is again in evidence with positive values seen above $y/D = 0.5$ and negative below. Although the asymmetry in this plane

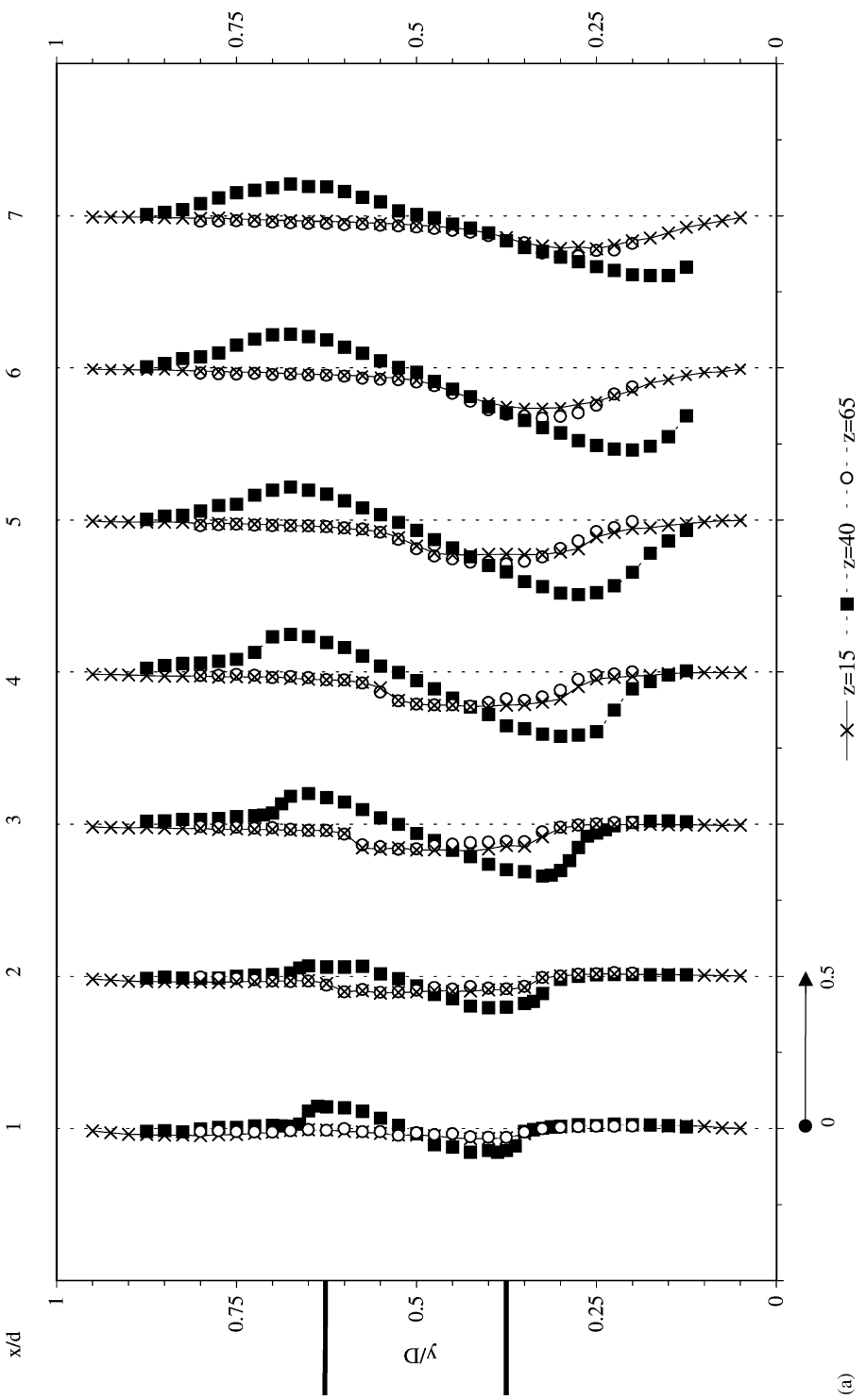

Fig. 8. (a and b) Mean transverse velocity (V/U_B) profiles.

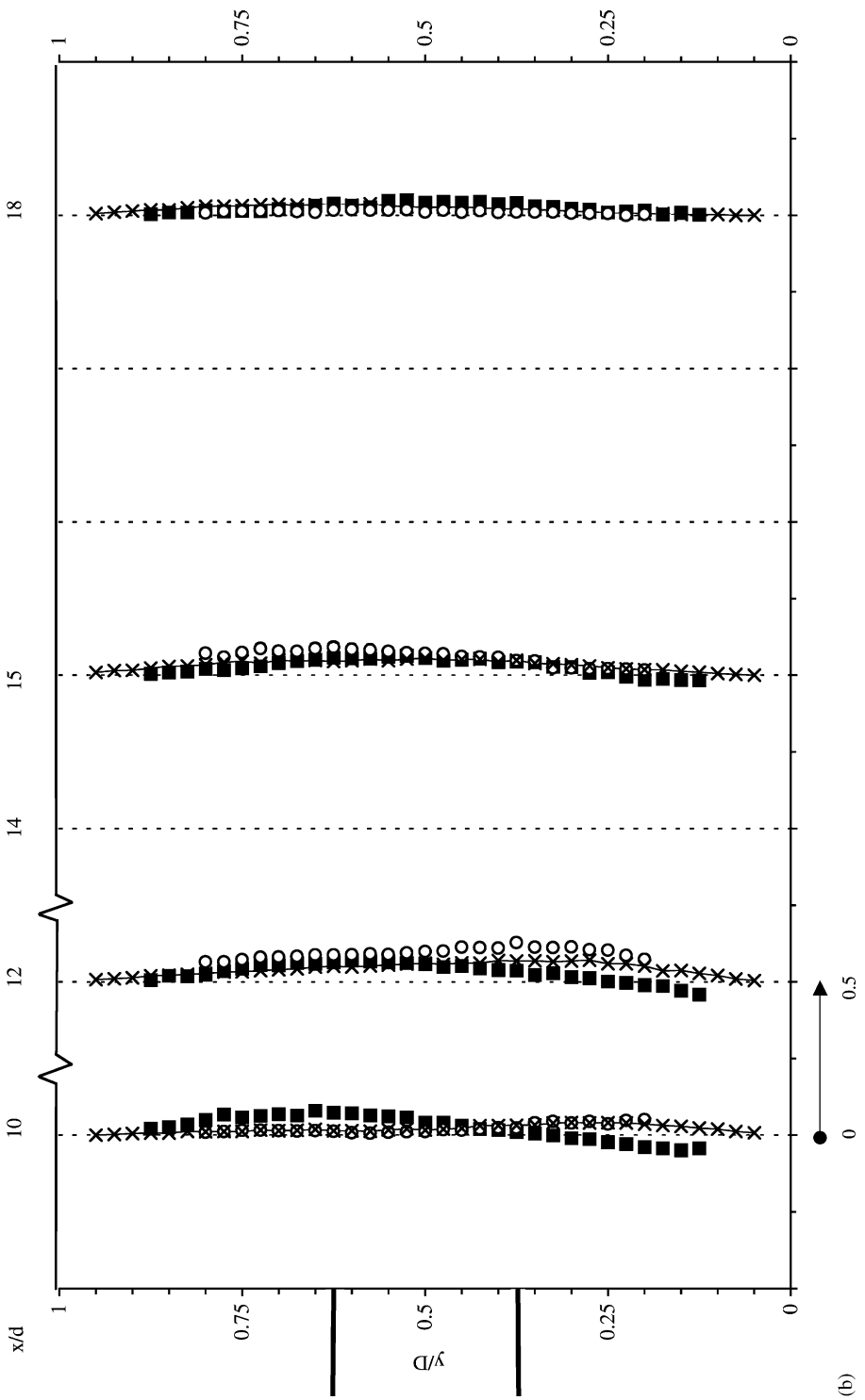

Fig. 8. (*Continued*).

is reduced it is not eliminated: the maximum positive transverse velocity is about $0.10\,U_B$, whereas the maximum negative value is approximately double at $0.21\,U_B$.

4.4. Streamwise turbulence intensity, u'/U_B

Fig. 9a and b show the normalised rms streamwise turbulence intensity u' with the low levels at $x/d = 0$ being a direct consequence of the smooth contraction immediately upstream of the expansion. For the water flow, this contraction geometry led to uniformly low turbulence intensity (circa 3%) across the duct [5]. For PAA, the situation is more complex. Along the *XY*-centreplane, the inlet intensity levels are roughly uniform at about $0.1\,U_B$: a significant increase compared to the water flow. The $z = 15$ and 65 mm profiles are in close agreement with each other and have a low intensity (circa 4%) core but exhibit a peak near the wall of about $0.12\,U_B$. In the near vicinity of the expansion ($x/d < 6$), the reduced top-to-bottom asymmetry for the flow along the *XY*-centreplane compared to the $z = 15$ and 65 mm profiles is again seen. Downstream of $x/d = 6$, the profiles along the *XY*-centreplane become increasingly asymmetric. In the lower recirculation region (i.e. below the high-velocity core), the maximum streamwise intensity is equal for the three profiles at $0.20\,U_B$, a reduction of about 10% compared to the water flow. Above the high-velocity core, all three maximum values are also slightly attenuated compared to the water flow: the $z = 15$ and 65 mm profiles have approximately equal values ($\approx 0.22\,U_B$), whereas the *XY*-centreplane data has a larger value of $0.25\,U_B$.

4.5. Transverse turbulence intensity, v'/U_B

The profiles of normalised rms transverse turbulence intensity are shown in Fig. 10a and b and are similar in shape to those of the streamwise turbulence intensity but are greatly reduced in magnitude (note the reduced scale of Fig. 10 compared to Fig. 9). In the very near vicinity of the expansion, $x/d < 2$, there is no discernible peak in the transverse intensity distributions. The reduction in magnitude compared to both their streamwise counterparts and the equivalent water values is large: the maximum transverse intensity is less than half the streamwise value. Such high levels of turbulence anisotropy is consistent both with the data reported in [2] and with previously reported drag-reduction studies [14,15], where the transverse intensity is always attenuated. In drag-reduction studies, the effect on the streamwise intensity is rather mixed: an increase is usually observed when normalised by the *friction* velocity. Whereas, when normalised by the bulk velocity (as in the current study) the trend is not so apparent or general: depending on the type of polymer, the maximum values can be increased, decreased, or remain approximately the same as in the Newtonian case.

4.6. Reynolds shear stress, $\overline{uv}/U_B^2$

The distributions of normalised Reynolds shear stress $\overline{uv}$ are shown in Fig. 11a and b. As would be expected from the transverse turbulence-intensity measurements, the magnitude of the Reynolds shear stress is also greatly reduced compared to water. Also compared to the equivalent water results [5], the region of high Reynolds shear stress (i.e. within the shear layer) is narrower. In the lower recirculation region along the *XY*-centreplane, the maximum shear stress is only $0.01\,U_B^2$, less than half the Newtonian value, and in the upper recirculation region it is of opposite sign (as expected from the sign of the velocity gradient) and smaller again at $0.045\,U_B^2$. The $z = 15$ and 65 mm profiles have Reynolds shear stresses of

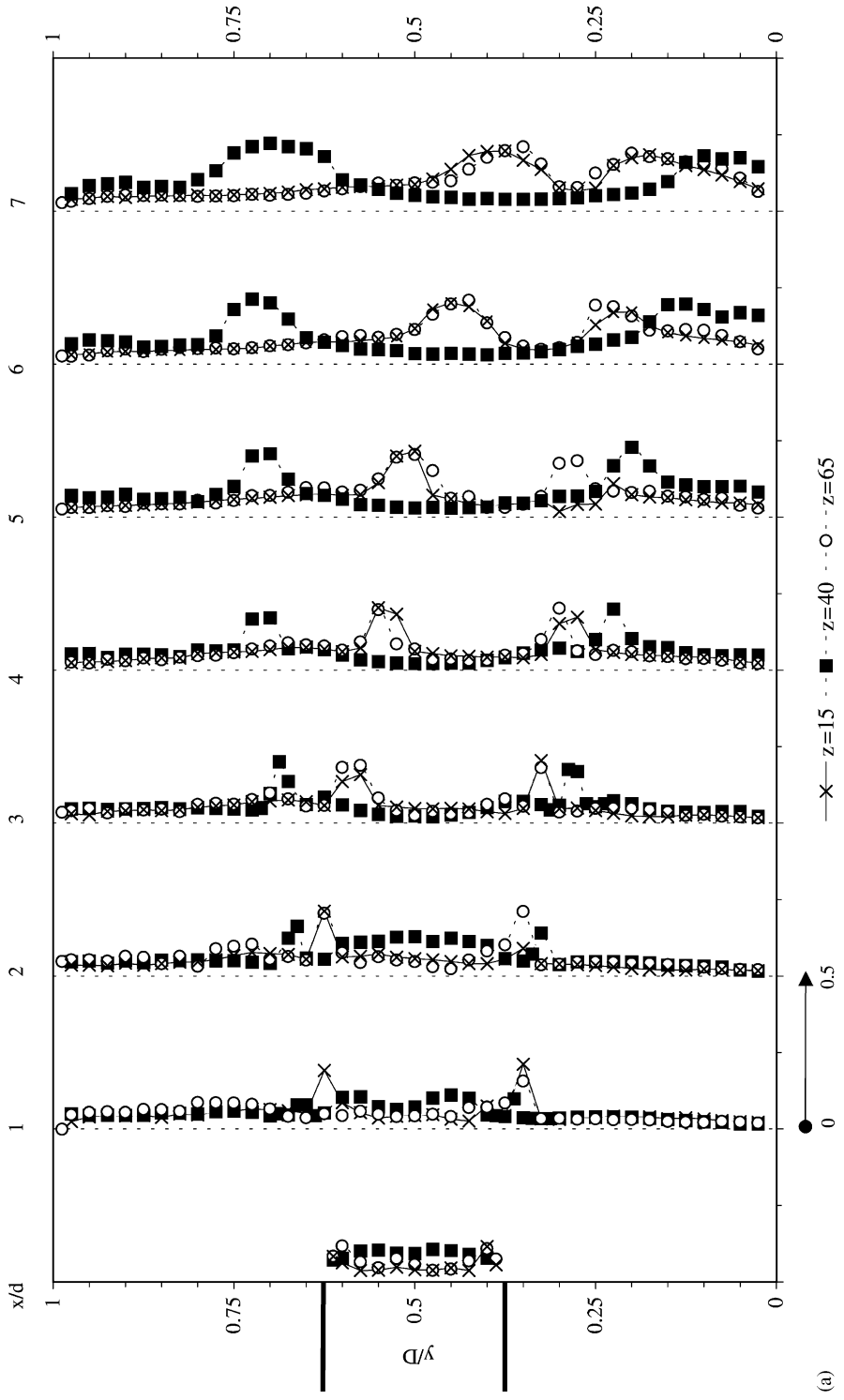

Fig. 9. (a and b) Streamwise turbulence intensity (u'/U_B) profiles.

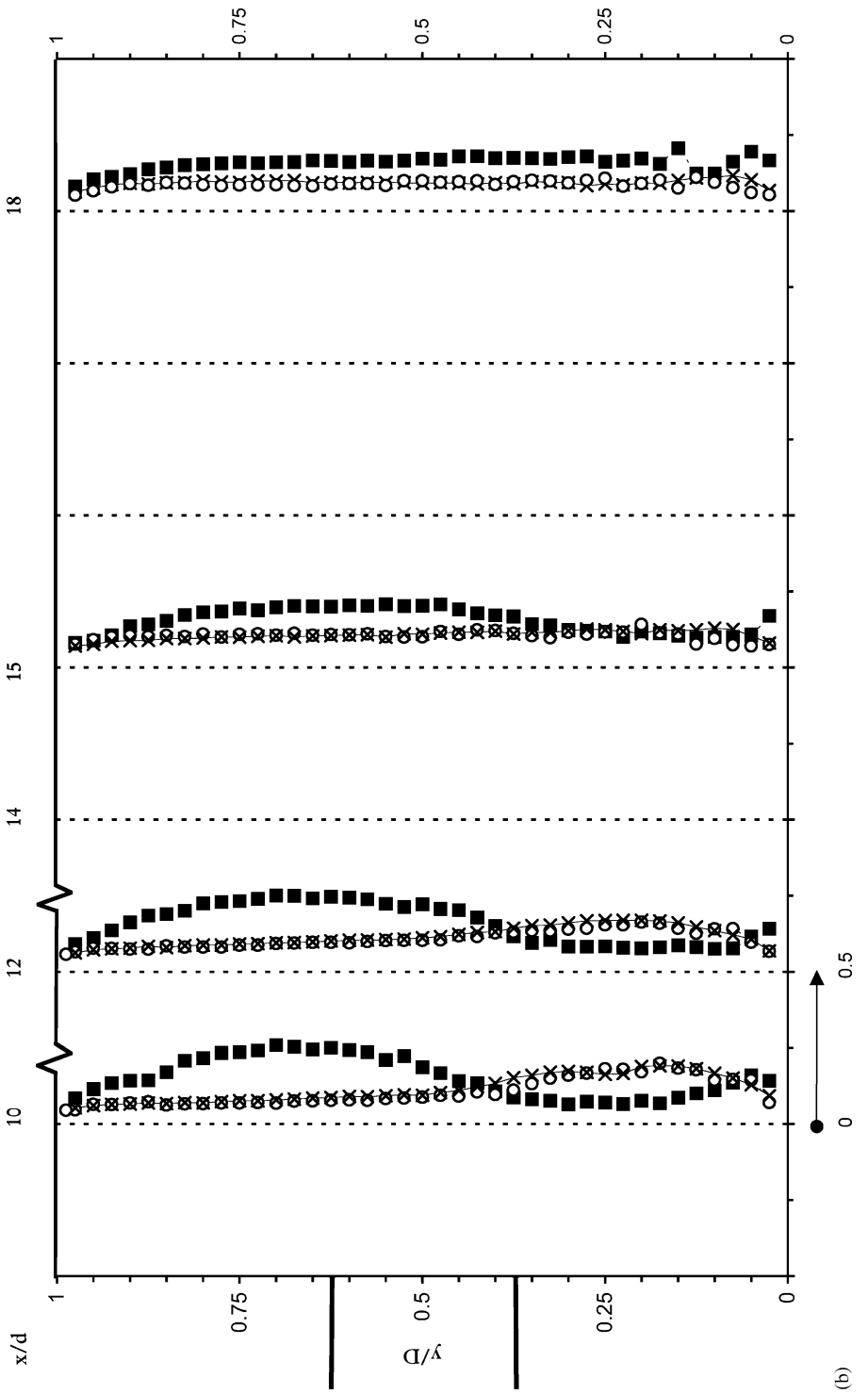

Fig. 9. (*Continued*).

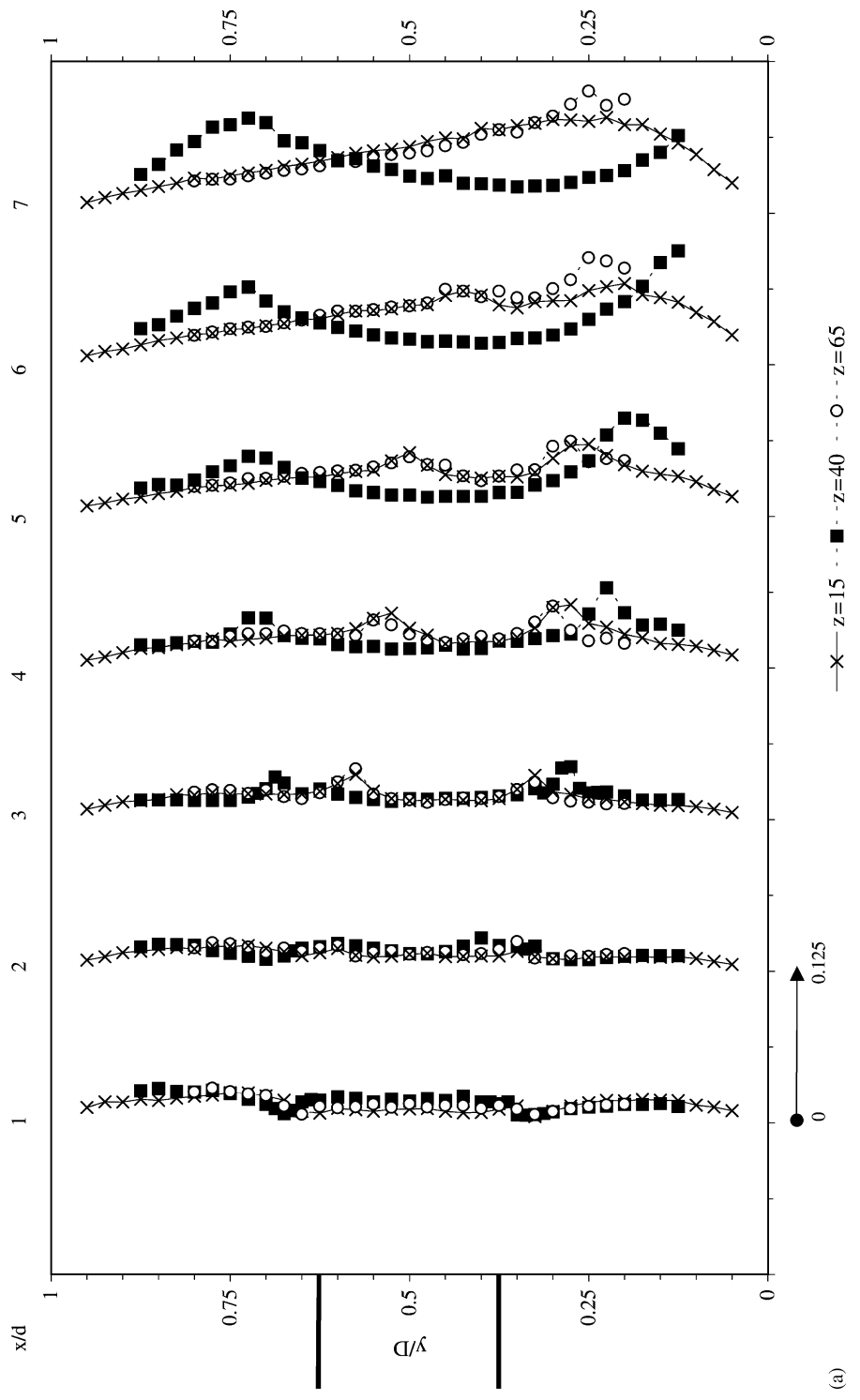

Fig. 10. (a and b) Transverse turbulence intensity (v'/U_B) profiles.

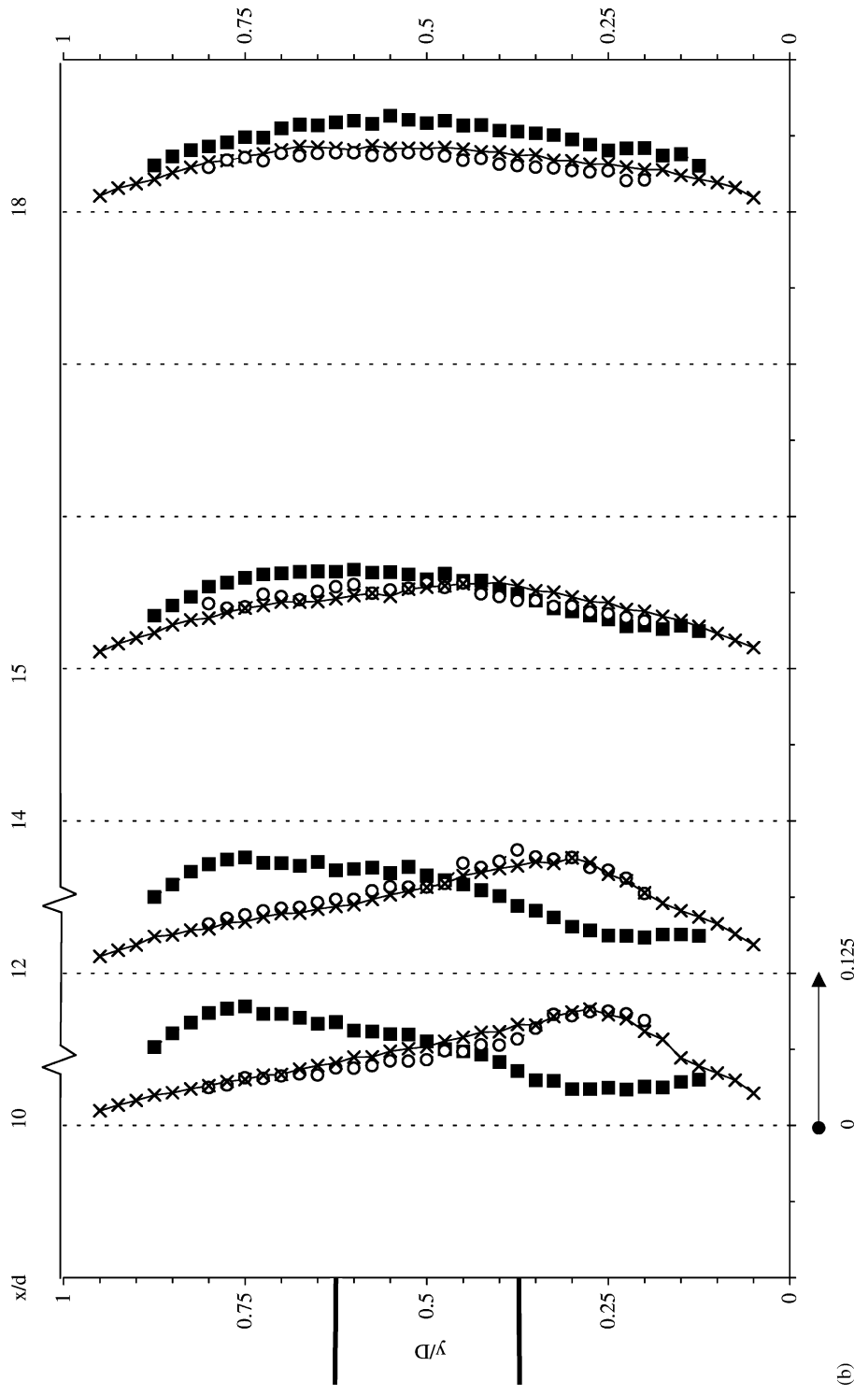

Fig. 10. (*Continued*).

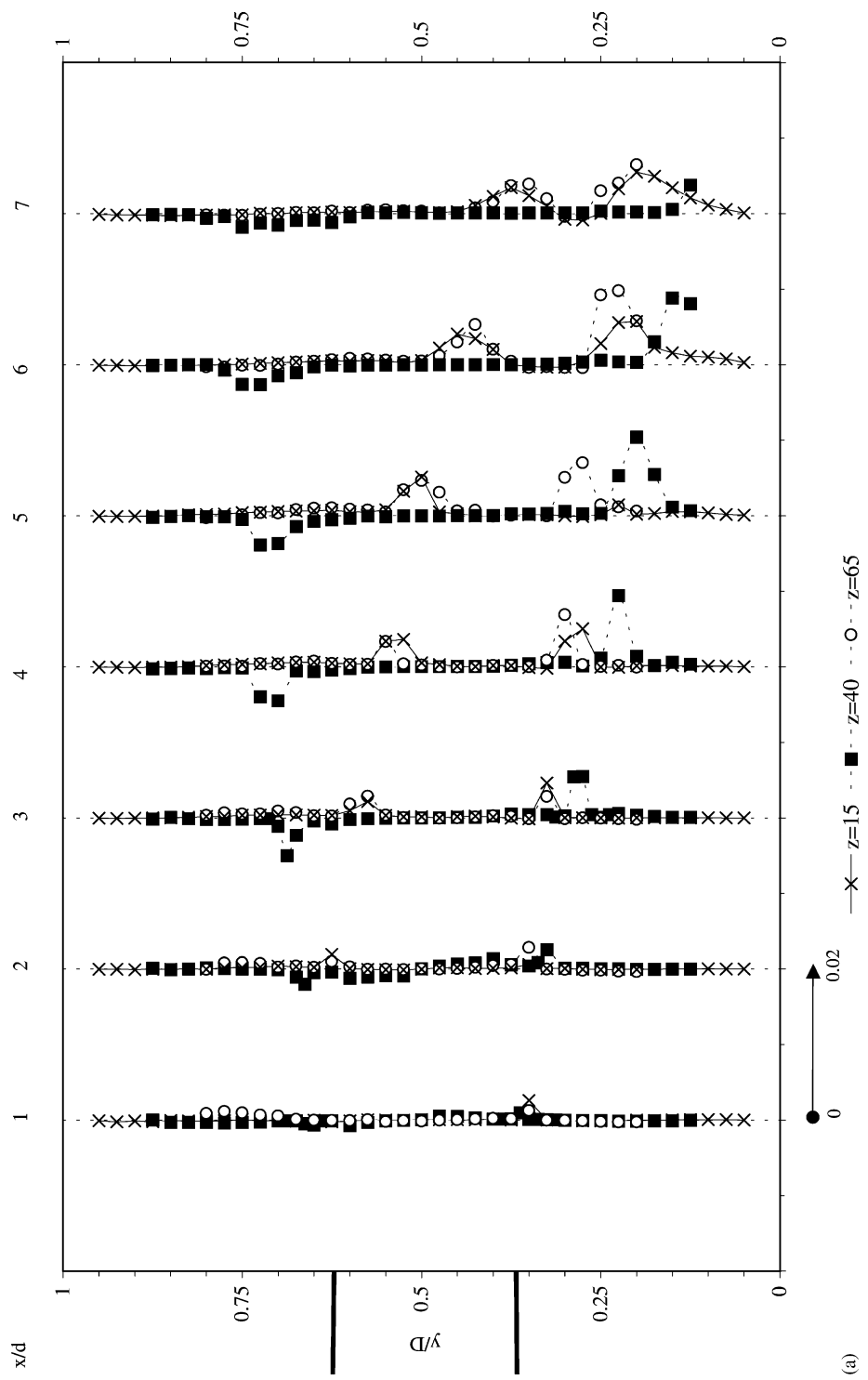

Fig. 11. (a and b) Reynolds shear stress ($-\overline{uv}/U_B^2$) profiles.

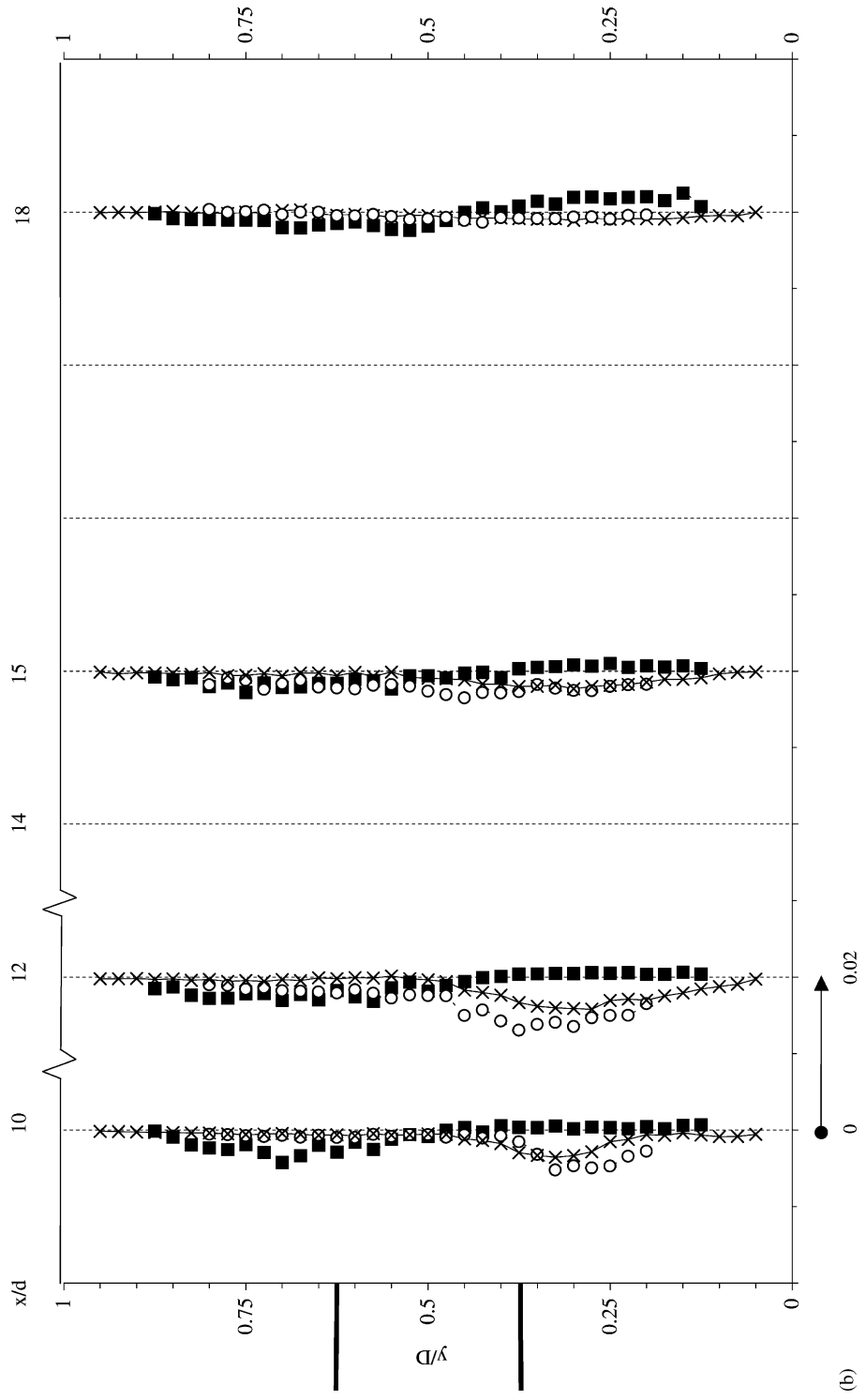

Fig. 11. (*Continued*).

the same sign in both the lower and upper recirculation regions and this is a consequence of the negative transverse velocities present both above and below the high-velocity core (see Fig. 8a). Once again, the maximum values of Reynolds shear stress for these planes are also greatly reduced compared to the water flow.

5. Conclusions

Results have been reported for the turbulent flow of a 0.125% concentration of PAA at a Reynolds number of 13,700 through a plane sudden expansion of expansion ratio 4 and aspect ratio 5.33 at 3 spanwise and 12 streamwise locations. For this viscoelastic and shear-thinning fluid, the modest aspect ratio produces a flow that is both far from two dimensional and fundamentally different to the flow of water through the same geometry. Along the *XY*-centreplane, the top-to-bottom asymmetry seen in water flows is initially ($x/d < 6$) diminished although not eliminated as is evident from the presence of recirculating fluid below the high-velocity core but not above it. Downstream of $x/d = 6$, the flow becomes increasingly asymmetric with downstream distance. The apparent flowrate along the *XY*-centreplane increases with downstream distance until reaching a maximum almost three times the expected true flowrate at $x/d = 7$. It is speculated that this is a normal-stress effect. In the $z = 15$ and 65 mm planes, upstream of $x/d = 5$, the flow is approximately symmetric about the *XY*-centreplane but substantially different to the flow along the *XY*-centreplane. The flowfield is strongly very three dimensional and complex. Downstream of this location ($x/d = 5$) the side-to-side symmetry disappears and the underlying physics of the flowfield become even more complex. It is suggested that an aspect ratio much larger than the recommended value of 10 for a Newtonian fluid would be required for two-dimensional flow to result for a sudden expansion for viscoelastic liquids exhibiting large values of N_1/τ.

The maximum turbulence intensities are consistent with previously reported data for drag-reducing viscoelastic liquids. The maximum streamwise turbulence intensities are only slightly affected and in this case are reduced by about 10% compared to the Newtonian values.

The transverse component of velocity fluctuation is significantly reduced in both the lower (by about 50%) and upper (by about 30%) 'recirculation' regions. The maximum Reynolds shear stress $\overline{uv}$ is also significantly reduced, to a value about 50% lower than the corresponding water value.

References

[1] R.J. Poole, M.P. Escudier, Turbulent flow of non-Newtonian liquids over a backward-facing step. Part I. A thixotropic and shear thinning liquid, J. Non-Newtonian Fluid Mech. 109 (2003) 177.
[2] R.J. Poole, M.P. Escudier, Turbulent flow of non-Newtonian liquids over a backward-facing step. Part II. Viscoelastic and shear-thinning liquids, J. Non-Newtonian Fluid Mech. 109 (2003) 193.
[3] D.E. Abbott, S.J. Kline, Experimental investigation of subsonic turbulent flow over single and double backward-facing steps, J. Basic Eng. D 84 (1962) 317.
[4] J.K. Eaton, J.P. Johnston, A review of research on subsonic turbulent flow reattachment, AIAA J. 19 (1981) 1093.
[5] M.P. Escudier, P.J. Oliveira, R.J. Poole, Turbulent flow through a plane sudden expansion of modest aspect ratio, Phys. Fluids 14 (2002) 3641.
[6] P. Townsend, K. Walters, Expansion flows of non-Newtonian liquids, Chem. Eng. Sci. 49 (1994) 749.
[7] M.S. Darwish, J.R. Whiteman, M.J. Bevis, Numerical modelling of viscoelastic liquids using a finite-volume method, J. Non-Newtonian Fluid Mech. 45 (1992) 311.

[8] K.A. Missirlis, D. Assimacopoulos, E. Mitsoulis, A finite volume approach in the simulation of viscoelastic expansion flows, J. Non-Newtonian Fluid Mech. 78 (1998) 91.
[9] A. Baloch, P. Townsend, M.F. Webster, On vortex development in viscoelastic expansion and contraction flows, J. Non-Newtonian Fluid Mech. 65 (1996) 133.
[10] N. Phan-Thien, R.I. Tanner, A new constitutive equation derived from network theory, J. Non-Newtonian Fluid Mech. 2 (1977) 353.
[11] M.P. Escudier, S. Smith, Fully developed turbulent flow of non-Newtonian liquids through a square duct, Proc. R. Soc. Lond., Ser. A 457 (2001) 911.
[12] C. Tropea, Laser Doppler anemometry: recent developments and future challenges, Measur. Sci. Technol. 6 (1995) 605.
[13] W.J. Yanta, R.A. Smith, Measurements of turbulence-transport properties with a laser-Doppler velocimeter, in: Proceedings of the 11th Aerospace Science Meeting, Washington, AIAA paper 73, 1978, p. 169.
[14] M.P. Escudier, F. Presti, S. Smith, Drag reduction in the turbulent pipe flow of polymers, J. Non-Newtonian Fluid Mech. 81 (1999) 197.
[15] J.M.J. den Toonder, M.A. Hulsen, G.D.C. Kuiken, F.T.M. Nieuwstadt, Drag reduction by polymer additives in a turbulent pipe flow: numerical and laboratory experiments, J. Fluid Mech. 337 (1997) 193.
[16] J.R. Stokes, L.J.W. Graham, N.J. Lawson, D.V. Boger, Swirling flow of viscoelastic fluids. Part 1. Interaction between inertia and elasticity, J. Fluid Mech. 429 (2001) 67.
[17] K. Walters, A.Q. Bhatti, N. Mori, The influence of polymer conformation on the rheological properties of aqueous polymer solutions, in: D. De Kee, P.N. Kaloni (Eds.), Recent Developments in Structured Continua, vol. 2, Pitman, London, 1990.
[18] K. Yasuda, R.C. Armstrong, R.E. Cohen, Shear flow properties of concentrated solutions of linear and star branched polystyrenes, Rheol. Acta 20 (1981) 163.
[19] M.P. Escudier, I.W. Gouldson, A.S. Pereira, F.T. Pinho, R.J. Poole, On the reproducibility of the rheology of shear-thinning liquids, J. Non-Newtonian Fluid Mech. 97 (2001) 99.
[20] H.A. Barnes, J.F. Hutton, K. Walters, An Introduction to Rheology, Elsevier, Amsterdam, 1989.
[21] R.B. Bird, R.C. Armstrong, O. Hassinger, Dynamics of polymeric liquids, in: Fluid Mechanics, vol. 1, Wiley, New York, 1997.
[22] K.C. Tam, C. Tui, Improved correlation for shear-dependant viscosity of polyelectrolytes, J. Non-Newtonian Fluid Mech. 46 (1993) 275.
[23] S.E. Smith, Turbulent duct flow of non-Newtonian liquids, Ph.D. Thesis, Department of Engineering, The University of Liverpool, 2000.
[24] F. Presti, Investigations of transitional and turbulent pipe flow of non-Newtonian liquids, Ph.D. Thesis, Department of Engineering, The University of Liverpool, 2000.
[25] B. Yesilata, A. Oztekin, S. Neti, J. Kazakia, Pressure measurements in highly viscous and elastic fluids, J. Fluid Eng. 122 (2000) 626.
[26] R.J. Poole, M.P. Escudier, Laminar viscoelastic flow through a plane sudden expansion, in: Proceedings of the Eleventh International Symposium on Applications of Laser Techniques to Fluid Mechanics, Paper 31-4, 8–11 July, Lisbon, Portugal, 2002.
[27] V. de Brederode, P. Bradshaw, Three-dimensional flow in nominally two-dimensional separation bubbles. I. Flow behind a rearward facing step, Aero Rep. 72–19, Imperial College of Science and Technology, London, UK, 1972.